Assembly of Carbon Nanotubes on Polymer Particles: Towards Rapid Shape Change by Near-Infrared Light

*Xiaopeng Huang, Qiuping Qian, Xinyue Zhang, Wenbin Du, Huaping Xu, and Yapei Wang**

Particular shapes assist numerous natural micro-organisms and cells to survive in vivo by overcoming biological barriers. With this inspiration, shape is becoming an important factor for the design of new drug carriers.[1] In contrast to spherical particles, long cylindrical micelles show prolonged circulation that is considered due to their filamentous shape.[2] Another study reveals that unfavorable phagocytosis is observed to ellipsoidal particles along the short axis while quick phagocytosis happens along the long axis.[3] Soft particles with disc shape behave like red blood cell, displaying less clearance by macrophage and thus increasing the circulation time in vivo.[4] Growing drug delivery studies evidently reflect the importance of shape effect. This shape knowledge in biomaterial design is currently expanded to the fabrication of smart polymeric particles that are capable of changing shapes on demand. Shape change can enable highly elaborate function of controllable cellular interactions, providing a platform for prolonged circulation and targeted accumulation.[5]

There are examples of shape changing particles, such as particles consisting of liquid crystal polymers that change shape by phase transition,[6] azobenzene-containing particles that become prolate by Ar^+ laser triggering,[7] self-assembled aggregates that switch the morphology by the introduction of charge-transfer interaction[8] or DNA,[9] shape memory particles that are responsive to temperature,[10] photo-induced shape changes caused by alteration of cross-link density within the particles,[11] as well as pH-induced shape change of PLGA particles,[5] and photolysis-induced shape change peptide particles.[12] Regarding that most actuators are not appropriate for inherent application in vivo, many efforts have been devoted to developing near-infrared (near-IR) light-triggering biomaterials, as near-IR is considered less detrimental to healthy cells and can penetrate deeper into biological tissue. A traditional way to surmount this obstacle is to enable the materials to absorb light photons. This strategy is conducted by attaching the materials with specific chromophores that can absorb one- or two photons of near-IR light.[13] However, the conversion of straightforward light absorption to stimuli-response is generally slow and insufficient. Recently, up-conversion that coverts the near-IR light to higher-energy photons in the UV region,[14] and photothermal conversion that converts the light energy to heat afford great convenience to utilize near-IR light in various applications.[15] The former strategy limits to lanthanide-doped particles as upconverting agents, while the latter method serves as a versatile platform for outputting thermal stimulus by simply incorporating a wide range of actuators with capability of photothermal conversion, such as carbon nanotubes,[16] gold nanorods[17] or gold nanoshell,[18] into the thermal-responsive matrices.

In terms of potential biological applications, shape change triggered by near-IR light is extremely attractive, while the current research is still at infancy stage and successful examples are sparse. Herein, we propose a strategy to photothermally modulate shape change of sub-micrometer biodegradable particles in the near-IR spectral range. As a proof-of-concept, we coat single-wall carbon nanotubes (SWCNTs) onto a thermal-responsive polymer via a Pickering emulsion-based process. Heat generated by SWCNTs under near-IR irradiation rapidly melts the elongated particles, switching the shape from prolate to spherical because of the minimization of the interfacial energy.

The fabrication of biodegradable particles coated with SWCNTs is shown in **Figure 1**. A Pickering emulsion was formed between polycaprolactone (PCL, Mw ≈ 45000 g/mol) dissolved in dichloride methane and SWCNTs dispersed in water, in which polycaprolactone solution was the dispersed phase and the SWCNT solution was the continuous phase. Instead of traditional small molecular surfactants, SWCNTs acted as the emulsifier to stabilize the oil droplets in water. The dispersed PCL phase segregated and precipitated from the continuous phase due to heavier density of dichloride methane than water. A distinct feature of the precipitation is that SWCNTs are simultaneously transferred from continuous phase to the dispersed phase, suggesting that SWCNTs contributed to stabilization of Pickering emulsion. To prevent the coalescence of oil droplets during the organic solvents drying process, the as-synthesized Pickering emulsion was poured into a polyvinyl alcohol (PVA, MW ≈ 12000 g/mol) aqueous solution, allowing a formation of an additional layer of PVA on particle surface. The sandwich structure of PCL-SWCNT-PVA leads to isotropic particle collapse during solvent evaporation.

SWCNTs are poorly soluble in most solvents. To enhance their solubility in aqueous solution, SWCNTs were functional-

X. Huang, Q. Qian, X. Zhang, Prof. W. Du, Prof. Y. Wang
Department of Chemistry
Renmin University of China
Beijing, 100872, China
E-mail: yapeiwang@ruc.edu.cn
Prof. H. Xu
Department of Chemistry
Tsinghua University
Beijing, 100084, China

DOI: 10.1002/ppsc.201200130

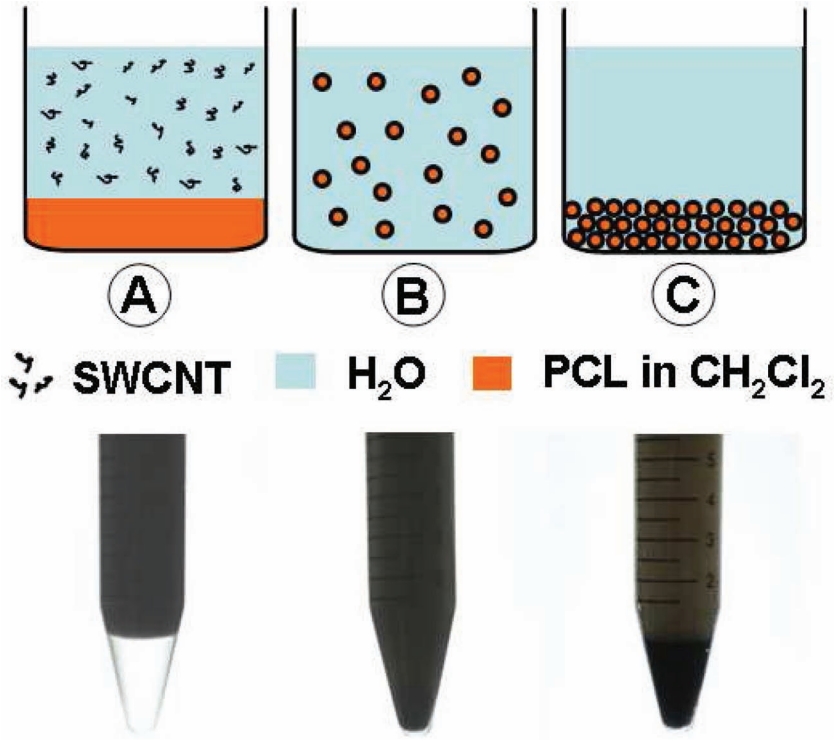

Figure 1. Preparation illustration of elongated near-IR-responsive particles: (A) Delamination of PCL dichloride methane solution and SWCNTs aqueous dispersion; (B) Pickering emulsion formed under stirring with an angular velocity of ×16 000 rpm; (C) The precipitation of PCL-CH_2Cl_2 droplets in the continuous phase. The concentration of SWCNTs is 0.05 mg/mL.

ized with carboxylic acid groups according to a previous procedure.[19] As shown in **Figure 2**a, carboxylated SWCNTs become well dispersed in water with ideal stability. Its wide absorbance across the entire spectrum is desirable for the efficient photothermal conversion. As a control, no absorbance signal was observed for untreated SWCNTs since they were completely precipitated out of water. Transmission electron microscope (TEM) observation additionally reveals the good dispersion of SWCNTs, as no evident aggregation exists. SWCNTs are broken under the harsh treatment for introducing carboxylic acid groups. TEM observation elucidated the carboxylated SWCNTs had a broad range of length, from several dozen to several hundred nanometer, much smaller than the original length of 5–15 μm. The length decrease indeed favors the stabilization of Pickering emulsion, as smaller filaments are expected to orientate more easily at the interface to minimize interfacial energy. The interfacial activity of SWCNTs was followed by pendant drop test as shown in Figure **2**c. Typically, a water droplet containing SWCNTs with defined concentration was suspended from the end of a capillary in a hexane solution. The change of dynamic interfacial tension yielded

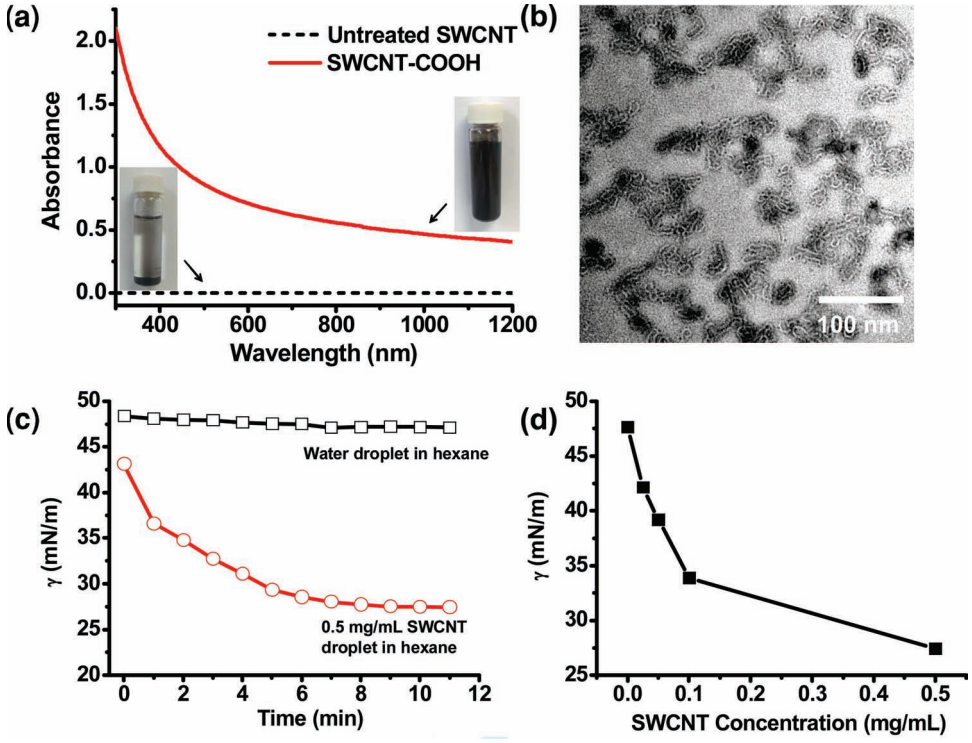

Figure 2. (a) UV-Vis absorbance of carboxylated SWCNT (0.1 mg/mL) aqueous solution in comparison to SWCNT aqueous solution without surface modification; (b) TEM observation of well-dispersed carboxylated SWCNT; (c) Dynamic interfacial tension between hexadecane and water by pendant drop method in the presence of SWCNT (0.5 mg/mL); (d) Dynamic interfacial tension between hexadecane and water upon increasing the SWCNT concentration in water.

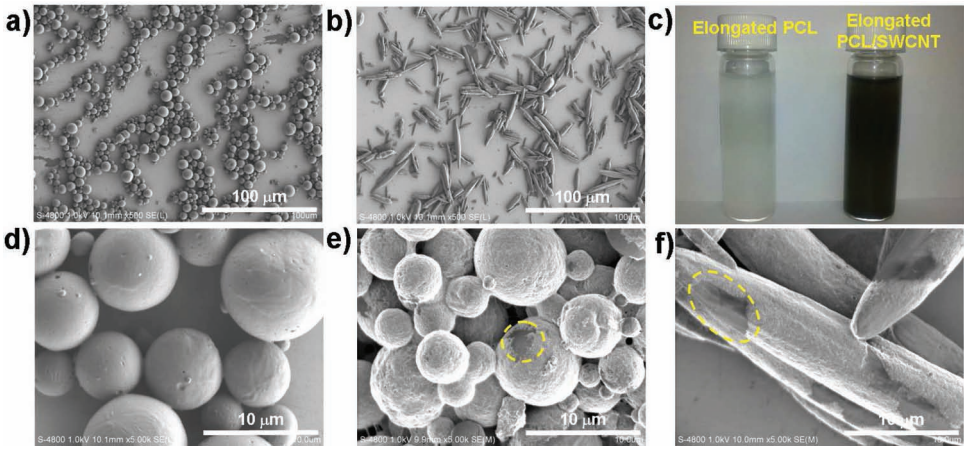

Figure 3. a) Free blank PCL particles without SWCNTs coating harvested from polyvinyl alcohol solution; b) Free elongated blank PCL particles without SWCNTs coating; c) The solutions of blank elongated PCL particles and elongated PCL particles with SWCNTs coating; d) SEM image of blank PCL particles; e) and f) SEM image of spherical and elongated PCL particles with SWCNTs coating, respectively. SEM images of a) and b) were captured using a lower detector; SEM images of d), e), and f) were captured by a mix detector. Marked regions represent surfaces without SWCNTs coating.

insight into the capability of particle adsorption at the water/oil interface. The interfacial tension between water and hexane was determined as 47.1 mN/m, while the interfacial tension between oil and water with 0.5 mg/mL SWCNTs dropped to 27.4 mN/m. Such an interfacial tension drop is attributed to surfactant-effect of SWCNTs at the interface. It should be noted that interfacial tension takes more than 10 minutes to reach equilibrium, elucidating a gradual migration process of SWCNTs from water phase to the interface. As shown in Figure 2d, the interfacial tension is also critically dependent on the SWCNT concentration. The increase of SWCNT concentration could induce more SWCNTs to be accumulated at the interface, which is envisioned to strengthen the photo-responsive ability of the resulting hybrid particles.

Solid PCL particles were generated by drying organic solvent. As shown in **Figure 3**a, spherical PCL particles with an average size of 10 μm were prepared in a high yield. Ellipsoidal PCL particles were produced via elongating the spherical PCL particles, according to some previous examples.[4b,5,20] Briefly, the oil droplets consisting of PCL polymer were redispersed in 5 wt% PVA aqueous solution, which was then dried to a thin elastic film. This thin film was elongated at high temperature over the melting point of PCL, engaging the particles to be stretched into a prolate shape. Free ellipsoidal particles were harvested by washing off the PVA, as shown in Figure **3**b. SWCNTs were well remained on the ellipsoidal PCL particles, which could be optically identified, as shown in Figure 3c. In comparison to blank elongated PCL particles without SWCNTs coating, particles coated with SWCNTs were remarkably dark. To discern the existence of SWCNTs on PCL particles, particles were carefully visualized by SEM using a mix-type detector which can reveal more surface details (Figure 3d-f). No SWCNTs were observed on blank PCL particle surface (Figure 3d), while a layer of SWCNTs exists on both spherical and elongated particle surface, as shown in Figure 3e and 3f. The particle surface coated with SWCNTs is relatively bright and easy to be focused as SWCNTs enable the particle surface conductive. Therefore, the SWCNTs coating regions are distinguished from the uncoated regions.

SWCNT is a photothermal-conversion agent in near-IR region. Localized temperature near the SWCNT surface by near-IR illumination can reach almost one thousand degree.[16a] The resulting heat is transferred to the surrounded environment, inducing a quick thermal response to the target material. As shown in **Figure 4**a, temperature of an aqueous solution con-

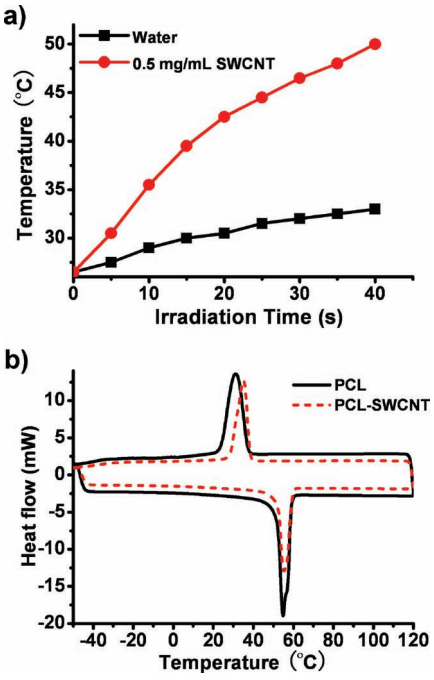

Figure 4. (a) The temperature change of water or SWCNTs aqueous dispersion (0.5 mg/mL) as a function of increasing near-IR exposure time; (b) Differential scanning calorimetry curves of blank PCL particles and SWCNTs-coated PCL particles.

Particle & Particle Systems Characterization
www.particle-journal.com

Materials Views
www.MaterialsViews.com

taining 0.5 mg/mL SWCNTs could be dramatically increased in a short-time near-IR exposure, while the temperature change of pure water induced by the thermal effect of near-IR is much smaller. The commercial available PCL (Mw ≈ 45000 g/mol) has a low glass transition temperature but it is typically crystallized. Melting point of this polymer was measured as 55 °C on a differential scanning calorimetry, which does not change upon coating SWCNTs on the surface of the polymeric particle (Figure 4b). As a result of phase transition, solid particles are transformed to liquid droplets when the temperature is over melting point, but it recovers to be solid if the temperature drops below the melting point. This easy thermal-induced phase transition paves the way to create a near-IR-responsive system by incorporating SWCNTs into the PCL matrix.

Shape change of elongated PCL particles relies on the availability of thermal-induced phase transition of PCL polymer. Ellipsoidal particles are envisioned to change the prolate shape to sphere at the liquid status because such a shape change can minimize the interfacial energy. The heat generated from SWCNTs coating by near-IR illumination is assumed to be quickly transported to PCL matrix of the particles, thus actuating the critical phase transition for shape change on demand. With this regard, elongated particles dispersed in aqueous solution were subjected to near-IR light illumination. The particle shape change was in-situ followed by an optical microscope. Notably, the photothermal conversion by SWCNTs plays a critical role in increasing the localized temperature to PCL particles. As shown in **Figure 5**c and 5d, an abrupt shape change of elongated SWCNTs-coated PCL particle occurs after 90 s near-IR light illumination. The response time of such a shape change by near-IR light illumination could be significantly shortened by coating more SWCNTs on PCL particles. PCL particles utilizing 0.15 mg/mL SWCNTs as the emulsifier rapidly underwent shape change after 25 s near-IR light illumination (Figure 5e and 5f). Additional in-situ movies are captured as shown in supporting information, demonstrating a whole shape change process via NIR illumination. In comparison, elongated PCL particles without SWCNTs coating are inert within the range of 300 s near-IR illumination, illustrating the thermal induced by light itself is negligible for a complete shape change, as shown in Figure 5a and 5b. A factor of light power is additionally assessed as the decrease of light power can eliminate the detrimental damage to healthy cells. However, impairing the light intensity prolongs the critical response time of shape change. The shape change of SWCNTs-coated particles in Figure 5e was fulfilled by 25 s near-IR light illumination with a power density of 17 W/cm^2, while it takes 60 and 180 s to finish the shape change if the light power density drops to 14 and 10 W/cm^2, respectively.

In summary, we have formulated a novel concept based on photothermal conversion in near-IR region to rapidly change particle shape on demand. A hybrid system having carbon nanotubes coating on the shell of the polymeric particle was constructed via Pickering emulsion route. Thermal generation from carbon nanotubes under light illumination actuates the phase transition, thus rapidly triggering shape change of particles. The combination of carbon nanotubes on polymeric particles apparently decreases the illumination dosage for the critical phase transition. Rapid shape change by near-IR light, combined with the ease of particle fabrication, opens an avenue to exploit smart materials, such as responsive drug delivery vehicles. More challenges about desirable size distribution, precise shape control, low-power light illumination, decrease of illumination dosage, and surface targeting may be solved through the deliberate utilizing other biocompatible polymers having lower phase transition temperature, and other smaller photothermal-conversion agents, e.g., gold nanorods, that can do easy surface functionaliztion as well as enable the fabrication of monodisperse Pickering emulsion.

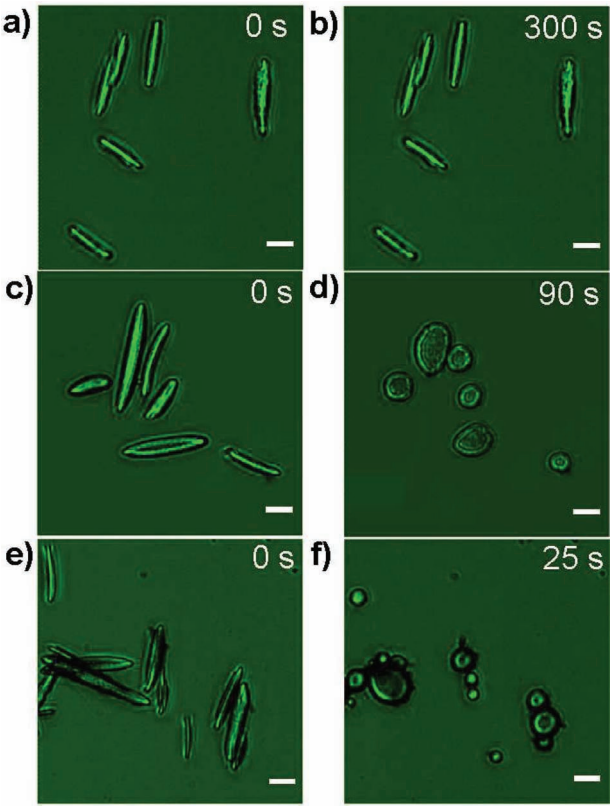

Figure 5. Microscopy images of PCL particles in aqueous solution. Elongated blank PCL particles (a) after near-IR light illumination for 300 s (b); Elongated PCL particles generated by using 0.05 mg/mL SWCNTs as the emulsifier (c) after near-IR light illumination for 90 s (d); Elongated PCL particles generated by using 0.15 mg/mL SWCNTs as the emulsifier (e) after Near-IR light illumination for 25 s (f). The distance between the near-IR laser (808 nm, 17 W/cm^2) and sample was set as 4 mm. Scale bar: 10 μm.

Experimental Section

Materials: Polycaprolactone (PCL, Mw~45000 g/mol) and polyvinyl alcohol (PVA, Mw~9000–10000 g/mol and ~12000 g/mol) were purchased from Sigma-Aldrich. Dichloromethane (DCM) was purchased from Beijing Chemical Reagent Company. Deionized water (18.2 MΩ/cm) was obtained from a Milli-Q water-purification system. SWCNT (95% purity, length 5–15 μm, inner diameter <2 nm) were purchased from Shenzhen Nanotech Port Co. Ltd and further oxidized with a mixture acid to obtain well water-dispersed fragments following a previously reported procedure.[19] Briefly, 10 mg SWCNTs were added to a 50 mL

of concentrated H_2SO_4/HNO_3 (3:1, 96% and 70%, respectively) solution and ultrasonicated in a water bath at 40°C for 24 h. The as-synthesized SWCNTs were subsequently centrifugated at 10000 rpm for 60 min three times and then washed with deionized water using polycarbonate filter (pore size 200 nm) to remove impurities. Finally, a carboxylated SWCNT (SWCNT-COOH) solution with weight concentration of 0.5 mg/mL was prepared for further application.

Characterization Methods: A commercial digital SLR camera (Nikon D3000) was employed to acquire some distinct and macroscopic pictures. Transmission electron microscope (JEMO 2010 electron microscope) was used to visualize the dispersibility of carboxylated SWCNT. Interfacial tension measurement was performed on a KSV Instruments LCD CAM 200 optical contact angle meter by pendant drop method at room temperature. A water droplet containing SWCNTs was suspended in hexane and the time-dependent surface tension was recorded per minute. Particles morphology was recorded on a scanning electron microscope (s-4800, Hitachi Co.) with an accelerating voltage of 1.0 KV. The light absorption behavior of carboxylated SWCNT was recorded on a UV-vis-NIR spectrometer (Lambda 750, Perkin-Elmer). Differential scanning calorimetry (DSC) measurements to determine the melting point of blank PCL particles and SWCNTs-coated PCL particles were performed on 5–10 mg samples under nitrogen atmosphere by using a Mettler Toledo 822e calorimeter. An 808 nm laser source (HTOE, Beijing, China), a fiber-coupled diode laser bar with a fiber of 1.0 m length and 400 μm core diameter, and a numerical aperture of 0.22, were used as the near-IR light-triggering source. The illumination power once emerging from the fiber end varied from 0 to 5 W depending proportionally on the current level from 0 to 2.0 A.

Preparation of Pickering Emulsion: The core-shell particles were prepared by using solvent evaporation method based on the Pickering emulsion. Typically, 1 mL PCL DCM solution (6.5 mg/mL) was mixed with 10 mL carboxylated SWCNTs aqueous solution (0.05 mg/mL or 0.15 mg/mL), followed by the addition of 0.5 mL PVA aqueous solution (0.02 wt%, Mw~9000–10000 g/mol) which act as a co-emulsifier with SWCNTs to stabilize the emulsion droplets. Mini-oil droplets were formed on a high shear emulsifier (Fluko FA25) under an angular velocity of 16, 000 rpm for 2 min. The Pickering emulsion eventually segregated and precipitated from the water phase. As a control, the blank PCL particles in the absence of SWCNTs were generated by the traditional emulsion method using neat PVA as the stabilizer.

Preparation of Elongated Particles: The precipitated emulsion was transferred into a film-forming solution containing 5 wt% PVA (Mw~12000 g/mol) and 2 wt% glycerol to prepare elongated particles via utilizing mechanically stretching method published previously with some modifications.[4b,5,20] Typically, 0.5 mL emulsion was added to 4 mL film-forming solution. The mixture was drop-cast onto a glass slide and dried into a solid film at room temperature. Accordingly, free spherical particles were prepared by dissolving the solid film (~35 mm). To prepare the elongated particles, a piece of solid film was mounted on an axial stretcher that comprises two aluminum blocks mounted on a screw which separates the blocks when turned. The film was stretched in air bath at 80 °C at a rate of 0.3–0.5 mm/s with a stretched ratio of 2.5. Free elongated particles would be obtained after the stretched film was removed and centrifuged at 8000 rpm for 5 min. Free particles were additionally washed with deionized water for five times to remove residual PVA. The above procedure was also applied to generate elongated blank PCL particles using precursor from traditional emulsion.

Near-IR Response: Photothermal conversion of SWCNTs was studied by reading temperature change of aqueous solution in the presence or absence of SWCNTs upon near-IR illumination. Temperature change of the solution which was filled in a circular polymer container was counted as function of light illumination time. The optical fiber end was maintained 4 mm away from the solution surface. A thermometer was used to measure the temperature of each solution at every time interval. Shape change of the elongated particles was captured on an inverted fluorescence microscope Eclipse Ti (Nikon, Japan) using a 20× objective lens equipped with a Photometrics CoolSNAP HQ^2 Interline CCD camera (Tucson, AZ) connected to Nikon NIS-Elements analysis software. The distance between the fiber end and the upper surface of coverslip was maintained 4 mm to get rid of the heating effect caused by near-IR itself. In addition, an Olympus BX51microscope was used to record the real-time and in-situ movies of the particles recovery under near-IR exposure with the help of Metamorph analysis software. In view of the very close space between the objective lens and the coverslip, the radiation model was kept at the direction of some 10 degrees and the distance of about 3 mm.

Acknowledgements

This work was financially supported by the Fundamental Research Funds for the Central Universities, and the Research Funds of Renmin University of China (20334010, 20473045, and 20574040). Mr. Jinchao He was acknowledged for his help to prepare water-dispersed SWCNTs.

Received: November 15, 2012

[1] a) S. Mitragotri, J. Lahann, *Nat. Mater.* **2009**, *8*, 15–23; b) R. A. Petros, J. M. DeSimone, *Nat. Rev. Drug Discov.* **2010**, *9*, 615–627; c) F.Zhao, Y. Zhao, Y.Liu, X. Chang, C. Chen, Y. Zhao, *Small* **2011**, *7*, 1322–1337.

[2] Y. Geng, P. Dalhaimer, S. S. Cai, R. Tsai, M. Tewari, T. Minko, D. E. Discher, *Nat. Nanotechnol.* **2007**, *2*, 249–255.

[3] J. A. Champion, S. Mitragotri, *Proc. Natl. Acad. Sci. USA* **2006**, *103*, 4930–4934.

[4] a) T. J. Merkel, S. J. Jones, K. P. Herlihy, F. R. Kersey, A. R. Shields, M. E. Napier, J. C. Luft, H. Wu, W. C. Zamboni, A. W. Wang, J. E. Bear, J. M. DeSimone, *Proc. Natl. Acad. Sci. USA* **2011**, *108*, 586–591; b) N. Doshi, A. S. Zahr, S. Bhaskar, J. Lahann, S. Mitragotri, *Proc. Natl. Acad. Sci. USA* **2011**, *108*, 586–591.

[5] a) J.-W. Yoo, S. Mitragotri, *Proc. Natl. Acad. Sci. USA* **2010**, *107*, 11205–11210; b) N. Daum, C. Tscheka, A. Neumeyer, M. Schneider, *WIREs Nanomed. Nanobiotechnol.* **2012**, *4*, 52–65; c) J. A. Champion, Y. K. Katare, S. Mitragotri, *J. Controlled Release* **2007**, *121*, 3–9.

[6] a) Z. Q. Yang, W. T. S. Huck, S. M. Clarke, A. R. Tajbakhsh, E. M. Terentjev, *Nat. Mater.* **2005**, *4*, 486–490; b) C. Ohm, N. Haberkorn, P. Theato, R. Zentel, *Small* **2011**, *7*, 194–198; c) S. Haseloh, C. Ohm, F. Smallwood, R. Zentel, *Macromol. Rapid Commun.* **2011**, *32*, 88–93.

[7] a) Y. B. Li, Y. N. He, X. L. Tong, X. G. Wang, *J. Am. Chem. Soc.* **2005**, *127*, 2402–2403; b) Y. B. Li, X. L. Tong, Y. N. He, X. G. Wang, *J. Am. Chem. Soc.* **2006**, *128*, 2220–2221; c) B. Liu, Y. He, X. G. Wang, *Langmuir* **2006**, *22*, 10233–10237.

[8] C. Wang, S. C. Yin, S. L. Chen, H. P. Xu, Z. Q. Wang, X. Zhang, *Angew Chem. Int. Ed.* **2008**, *47*, 9040–9052.

[9] M.-P. Chien, A. M. Rush, M. P. Thompson, N. C. Gianneschi, *Angew. Chem. Int. Ed.* **2010**, *49*, 5076–5080.

[10] S. M. Brosnan, Y. Wang, V. S. Ashby, **2012**, submitted.

[11] D. Klinger, K. Landfester, *Soft Matter* **2011**, *7*, 1426–1440.

[12] T. Muraoka, C.-Y. Koh, H. Cui, S. I. Stupp, *Angew. Chem. Int. Ed.* **2009**, *48*, 5946–5949.

[13] a) J. Fablan, *Chem. Rev.* **1992**, *92*, 1197–1226; b) J. Babin, M. Pelletier, M. Lepage, J.-F. Allard, D. Morris, Y. Zhao. *Angew. Chem. Int. Ed.* **2009**, *48*, 3329; c) Q. Lin, Q. Huang, C. Li, C. Bao, Z. Liu, F. Li, L. Zhu, *J. Am. Chem. Soc.* **2010**, *132*, 10645–10647.

[14] a) B. Yan, J.-C. Boyer, N. R. Branda, Y. Zhao, *J. Am. Chem. Soc.* **2011**, *133*, 19714–19717; b) R. Deng, X. Xie, M. Vendrell, Y.-T. Chang, X. Liu, *J. Am. Chem. Soc.* **2011**, *133*, 20168–20171; c) J. Zhou, Z. Liu, F. Li, *Chem. Soc. Rev.* **2012**, *41*, 1323–1349; d) Q. Liu, T. Yang, W. Feng, F. Li, *J. Am. Chem. Soc.* **2012**, *134*, 5390–5397.

[15] B. P. Timko, T. Dvir, D. S. Kohane, *Adv. Mater.* **2010**, *22*, 4925–4943.
[16] a) S. J. Pastine, D. Okawa, A. Zettl, J. M. J. Fréchet, *J. Am. Chem. Soc.* **2009**, *131*, 13586–13587; b) E. Miyako, H. Nagata, K. Hirano, T. Hirotsu, *Small* **2008**, *4*, 1711–1715 ; c) T. Fujigaya, T. Morimoto, Y. Niidome, N. Nakashima, *Adv. Mater.* **2008**, *20*, 3610–3614; d) E. Miyako, H. Nagata, K. Hirano, T. Hirotsu, *Small* **2008**, *4*, 1711–1715; e) Z. Zhang, L. Wang, J. Wang, X. Jiang, X. Li, Z. Hu, Y. Ji, X. Wu, C. Chen, *Adv. Mater.* **2012**, *24*, 1418–1423.
[17] a) I. Gorelikov, L. M. Field, E. Kumacheva, *J. Am. Chem. Soc.* **2004**, *126*, 15938–15939; b) M. Das, N. Sanson, D. Fava, E. Kumacheva, *Langmuir* **2007**, *23*, 196–201; c) T. Kawano, Y. Niidome, T. Mori, Y. Katayama, T. Niidome, *Bioconjugate Chem.* **2009**, *20*, 209–212; d) J. Kim, M. J. Serpe, L. A. Lyon, *Angew. Chem. Int. Ed.* **2005**, *117*, 1357–1360; e) K. C. Hribar, R. B. Metter, J. L. Ifkovits, T. Troxler, J. A. Burdick, *Small* **2009**, *5*, 1830–1834; f) Y.-T. Chang, P.-Y. Liao, H.-S. Sheu, Y.-J. Tseng, F.-Y. Cheng, C.-S. Yeh, *Adv. Mater.* **2012**, *24*, 3309–3314.
[18] a) H. Ke, J. Wang, Z. Dai, Y. Jin, E. Qu, Z. Xing, C. Guo, X. Yue, J. Liu, *Angew. Chem. Int. Ed.* **2011**, *50*, 3017; b) Y. Jin, X. Gao, *J. Am. Chem. Soc.* **2009**, *131*, 17774–17776; c) M. S. Yavuz, Y. Cheng, J. Chen, C. M. Cobley, Q. Zhang, M. Rycenga, J. Xie, C. Kim, K. H. Song, A. G. Schwartz, L. V. Wang, Y. Xia, *Nat. Mater.* **2009**, *8*, 935–939; d) H. Park, J. Yang, S. Seo, K. Kim, J. Suh, D. Kim, S. Haam, K.-H. Yoo, *Small* **2008**, *4*, 192–196.
[19] a) J. Liu, A. G. Rinzler, H. Dai, J. H. Hafner, R. K. Bradley, P. J. Boul, A. Lu, T. Iverson, K. Shelimov, C. B. Huffman, F. Rodriguez-Macias, Y.-S. Shon, T. R. Lee, D. T. Colbert, R. E. Smalley, *Science* **1998**, *280*, 1253–1256; b) Q. Liu, B. Chen, Q. Wang, X. Shi, Z. Xiao, J. Lin, X. Fang, *Nano Lett.* **2009**, *9*, 1007–1010.
[20] C. Herrmann, M. B. Bannwarth, K. Landfester, D. Crespy, *Macromol. Chem. Phys.* **2012**, *213*, 829–838.